Energy & Position Reconstruction on CsI (Tl) Scintillator Detector Array in TEXONO Experiment [*]

ZHU Yue-Feng[1;1)]   LI Yu-Lan[1]   Wong Henry Tsz-King[3]   LI Jin[1,2]   Venktesh. Singh[3]   Lin Shin-Ted[3]

1 (Department of Engineering Physics, Tsinghua University, Beijing 100084, China)
2 (Institute of High Energy Physics, CAS, Beijing 100049, China)
3 (Institute of Physics, AS, Taipei 11529, China)

Abstract   A high-Z nuclei detector based reactor neutrino spectra measurement is being operated by TEXONO collaboration, focusing on low energy low background experiments in neutrino and astroparticle physics. This article reviews the data processing procedures adopted on CsI(Tl) scintillator detector array, one of the two major detectors in TEXONO project. Owing to the complications in reconstructing energy spectra from the two-end output system, two approaches are introduced to improve the resolution of the final result.

Key words   reactor neutrino, CsI(Tl) crystal, resolution improvement

1   Introduction

TEXONO[2)] experiment is a reactor neutrino experiment based on solid detectors rather than liquid scintillator techniques, which has been deployed in this domain for many years, while the use of solid detectors such as CsI(Tl) scintillator is still at the beginning stage. An array of 93 CsI(Tl) crystals, weighting as a sum 186 kg, and a 1-kg ultra low background high purity germanium (ULB-HPGe) detector have been built in Kuo-Sheng Nuclear Power Plant[1,2] located at the northern coast of Taiwan. These two detectors aim at measuring the cross section for the process of electron antineutrino-electron scattering (ν_e e) of reactor neutrino.

$$\nu_e + e^- \rightarrow \nu_e + e^- . \qquad (1)$$

The process of ($\bar{\nu}_e$ e) scattering provides experimental approaches to identify the electro-weak parameters (g_V, g_A and $\sin^2 \theta_W$) of the Standard Model, as well as one of the most realistic measurements for searching the interference effects between Z and W exchanges[3]. In the previous experi-

ments, the measurement on accelerators with high energy (GeV) neutrino has achieved an accuracy of 3% for $\sin^2 \theta_W$ and g_A, mostly associated with ν_μ and ν_μ[4,5], whereas the ($\bar{\nu}_e$ e) scattering thought they have been observed with the accuracy in a range of 30%—50% for the cross section, thus the $\sin^2 \theta_W$[6—8], has not been well measured. Therefore the solid conclusion, for example, of W-Z interference[3], is not available now. Additionally, The cross section of the reaction is sensitive to study the neutrino magnetic moments (μ_ν)[9]. Fig. 1(a) depicts the cross section of ($\bar{\nu}_e$ e) scattering expected by the Standard Model and due to the neutrino magnetic moment of 10^{-10} μ_B as well as the case of coherent $\bar{\nu}_e$-N scattering. A detailed formulation shows the $1/T$ dependence on the magnetic moment term, indicating the requirement of low energy threshold (say, 1MeV or less) in the investigations for μ_ν. A recent report[10] gives a detailed discussion about the merits of detecting the derivation from the Standard Model by precisely measuring the cross section. Therefore, experiments on reactor neutrino with low threshold are hopeful

to provide an opportunity of exploring electro-weak physics at MeV scale and looking for small neutrino magnetic moment.
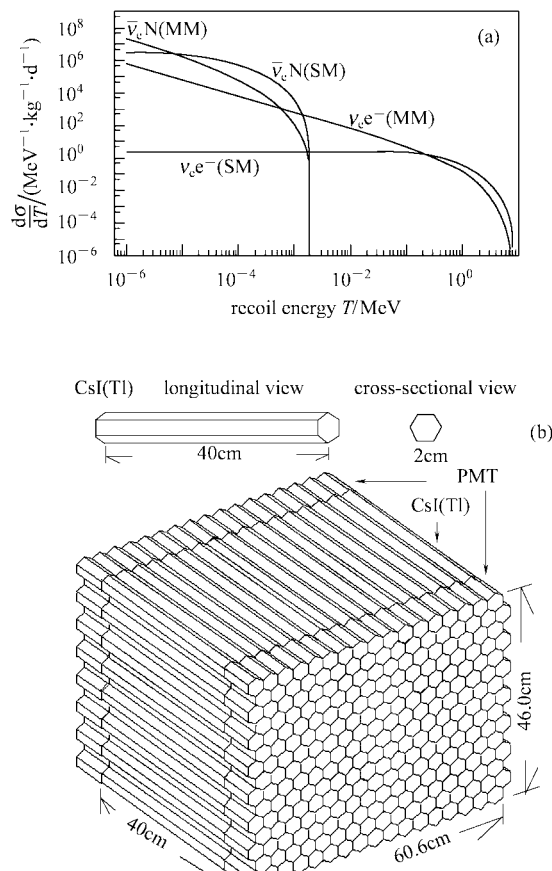

Fig. 1. (a) Differential cross section based on the Standard Model and due to a neutrino magnetic moment of 10^{-10} μ_B, for $\bar{v}_e$-e and coherent $\bar{v}_e$-N scattering, at a reactor neutrino flux of 10^{13} $cm^{-2} \cdot s^{-1}$; (b) Configuration of CsI(Tl) scintillator detector array. This detector consists of 93 2-kilogram crystals weighting as a sum 186 kg.

Further taking into account of the limitation of spectra measurements derived from the uncertainty of modeling low energy reactor neutrino spectra[11], the ranges of above 1.5MeV and below 100keV in the spectra are set to be the purpose of TEXONO, measured by the CsI(Tl) detector array and the ULB-HPGe detector respectively. A physical result has been achieved recently on the ULB-HPGe detector and the neutrino magnetic moment $\mu_{v_e} < 1.3(1.0) \times 10^{-10}$ μ_B at 90(68)% confidence level (CL) was rendered[12]. This article will focus on the data analysis process on the CsI(Tl) scintillator detector array, especially the approaches to achieve better resolution of the reconstructed energy spectra.

In Section 2 the experimental setups of the on-site labo-

ratory and the detectors are given, and Section 3 describes the off-site data analysis process of rebuilding the energy spectra and the longitude position information. Due to the complications in energy reconstruction, two approaches of improving the resolution are presented and discussed in detail.

2　Experimental setup

TEXONO on-site lab is located 28 meters away from one of the two reactor cores and 102 meters away from the other. It lies at the bottom of the seven-storey reactor building, thus taking the over-burden concrete floors as effective heavy shielding against cosmic ray. The detector chamber is surrounded by the plastic scintillator veto detectors and the thick passive shielding including, from outside inward, 15cm of lead bricks, 5cm of steel, 25cm of boron-loaded polyethylene and 5cm of OFHC copper, forming a 4π shielding coverage (overall 50 tons) to suppress the ambient radioactivity, and leaving an "inner target" square space with the dimension of 100cm × 80cm × 75cm, designed to be capable of putting in both CsI(Tl) detector array and ULB-HPGe detector at the same time. Nitrogen is inflated to the inner space in order to reduce the radioactivity from Radon.

The DAQ system is constructed based on the 16-channel, 20MHz, 8bit Flash Digital-to-Analogy converter Modules (FADC), which provide a powerful capability to record the whole digitalized pulse shape and timing parameters of the relevant events. Meanwhile, as presented recently[13], a extended dynamic range rather than 8bit provided literally by FADC hardware can be achieved through some software algorithms based on the whole pulse shape information without much expenditure. The ULB-HPGe detector and the CsI(Tl) detector array share the same DAQ system while they are trigged differently.

The geometry of the CsI(Tl) crystal modules is a 40-meter-long hexagonal prismoid with a cross section of 2 cm sides. Every module is a single crystal or for a few cases, it consists of two 20-meter glued ones that are placed at the peripheric places of the detector array. PMTs are mounted at both ends of the crystal as photo-electron converters. Signals retrieved from the two PMTs are used to reconstruct the energy information and the longitude position (or z-position as we call it) of the events[14]. The configuration of CsI(Tl) detector array is depicted in Fig. 1(b).

3 Data analysis

The data analysis process is based on the digitalized pulses given by the FADC system. Integrated areas of the pulses recorded at the two ends of a crystal (Q_l and Q_r) are the origin of the information of the energy and the longitude position. The relationship between Q_l as well as Q_r and the location of the event can be expressed as follows, if assuming fluorescence decays along the crystal exponentially.

$$Q_l = Q_{1/2}e^{-\lambda z}, \tag{2}$$

$$Q_r = Q_{1/2}e^{-\lambda(L-z)}. \tag{3}$$

Here L represents the total length of the crystal and z is the position where the event happens. $Q_{1/2}$ is half of the total electric quantity as an isotropic presumption of the emission of the fluorescence.

Obviously, multiplying Q_l and Q_r together, the outcome will rule out its dependence on z-position and give a measurement of the energy directly, which provides merits in rebuilding energy information[15]. Therefore, a geometric mean value $Q_t = \sqrt{Q_l \times Q_r}$ is defined as the measurement of the deposited energy. The z-position is acquired by considering the variance of the ratio $R = (Q_l - Q_r)/(Q_l + Q_r)$. However, since the existence of the different gain of the two PMTs, normalized Q_l and Q_r are demanded instead of unprocessed ones to establish an approximate linear relation between the ratio R and the z-position, a database of the pre-calibration to energy spectra and the normalization parameter for z-position is built to support further diagnostic purpose. With the above definition, energy resolution of 10% and the position resolution of 2cm at 662keV have been achieved.

The effort to regenerate the electric quantity from saturated pulses of FADC readout[13] is utilized to extend the dynamic range. Reference pulses are yielded on relevant crystals by adding the unsaturated pulses together to erase the influence of electric noise as well as inherent statistical fluctuation of the signals. A three-order polynomial is adopted to model the relationship between the whole area and the partial area (the area below the maximum value of the dynamic range of the FADC hardware) of the reference pulse that is multiplied by factors to simulate pulses at different amplitudes. A program is written to do such jobs and the acquired reconstruction parameters are stored in the parameter database. Therefore, to any saturated pulse its true electric quantity can

be reconstructed accordingly.

Many cuts have been employed in data processing to suppress the background events: (1). Cosmic ray veto. The time difference of the triggers between the plastic veto detector outside the passive shielding and the inner detectors is recorded as vetotime to identify cosmic ray; (2). Single hit cut. ($\bar{\nu}_e$ e) scattering only produces signals with the characteristic of single crystal hit and single trigger (or overall, single hit). Therefore the numbers of the crystals and the PMTs involved in an event as well as the inspired triggers are collected to tag the neutrino events; (3). PSD cuts. The PSD capability of CsI(Tl) scintillator provides a powerful facility to differentiate γ/β events from α events at a precision of > 99% above 500keV. The discrimination is available even if the pulse is partially saturated[13]. Additionally, with the rich information FADC records, other events that are not desired or of abnormal pulse shape-double pulse, for example-can also be picked out with some complicated PSD means, such as the arithmetical combination of the average values from different parts of a pulse. Table 1 gives a summary of these cuts and their suppression factors.

Table 1. The employed cuts and their suppression factors on CsI(Tl) detector array.

cuts	suppression factor
cosmic ray veto	0.50*
single hit cut	0.83*
α cut & other PSD cuts	0.26†
zpos cut	0.51*‡

* Based on the data of the whole detector array. The values may be different to every crystal due to various positions and electric thresholds.

† Specified for the central crystal in the array.

‡ Veto length is 4cm for each end.

In Fig. 2, a distribution of Q_l versus Q_r and the corresponding energy versus z-position plot after the reconstruction are depicted. It can be seen that ^{137}Cs band is uniform along the crystal, implying ^{137}Cs isotope resides evenly inside the crystals, while the other two bands: ^{40}K and ^{208}Tl attenuate with the depth increasing, as the evidence of the ambient radioactivity. Meanwhile, the concentration of the events along the two edge of the profile shows that the bulk of the background is exterior and can be effectively impeded by a not large thickness of CsI(Tl) crystals. For this reason, another cut (zpos cut) of making the two ends of the crystals as veto detectors is adopted and at last proved to be effective.
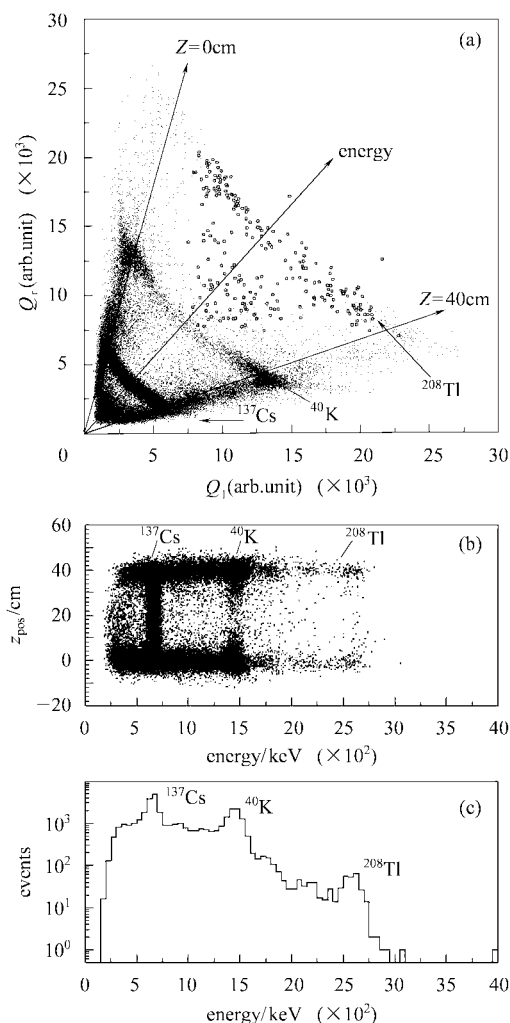
Fig. 2. (a) Distribution of Q_l versus Q_r, shows the events concentration of the background located in three bands that is related to ^{137}Cs, ^{40}K and ^{208}Tl and at the two ends of the crystal; (b) the distribution of z-position versus energy after reconstruction; (c) the spectrum of the background in one crystal with the data-taking for about 2 days.

4　Resolution improvement

As discussed in Section 3, energy can be reconstructed from PMTs' outputs Q_l and Q_r, and the rebuilt term is supposed to be irrelated to the longitude position of the event. Nevertheless, in many cases, the bands of ^{137}Cs, ^{40}K and ^{208}Tl seem not vertical or even not straight in the two-dimensional plot, indicating energy dependence on z-position, and as a result leading to the loss of the resolution in the energy spectra. Generally, there are two kinds of harmful relationship found between energy and z-position: slope and bend as

demonstrated in Fig. 3. ^{137}Cs band is shorter in these two plots than in Fig. 2 because of the threshold as marked by the broken line drawn in Fig. 3(b). Since the electronic threshold is made for Q_l and Q_r separately, as geometric mean value of them, energy must possess a triangle-shaped threshold in the 2-D plot. The following two subsections give a discussion of these profiles and two approaches are presented to neutralize them respectively.
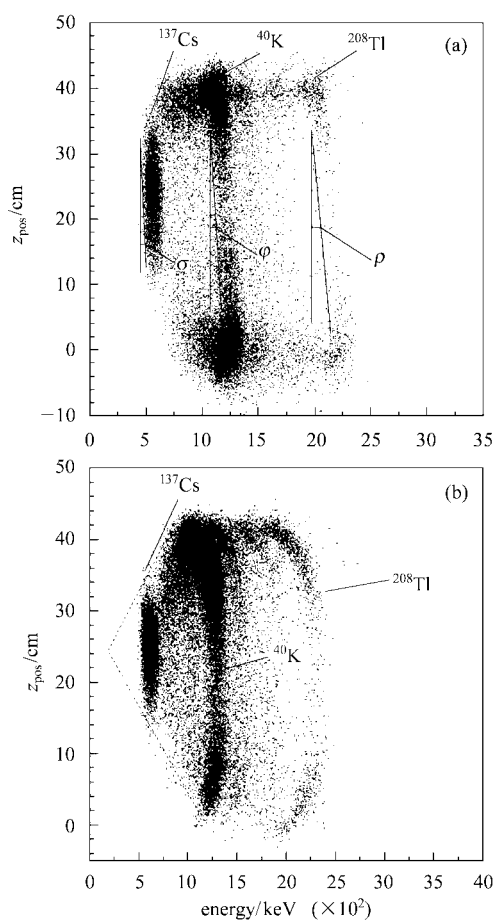

Fig. 3. (a) An example of slope profile. The difference among the bands' angles deviating from the verticality of the three isotopes is apparent; (b) A profile with bending bands, capable of decreasing the energy resolution at the low energy side of peaks. Both the above two figures do not calibrate their energy axis.

4.1　Slope compensation

The slopes of the three bands can be seen from Fig. 3 (a) and existence of them is able to cause damage to the resolution of the energy spectra. Actually, in a plot of z-position versus energy, the energy spectrum can be seen as the projection the plot makes to its x axis. Therefore, a slant band produces a peak wider than the width of the band itself which

is supposed to be the true resolution the peaks are.

The three angles between the bands and the vertical direction are represented by σ, φ and ρ. An increasing relationship among them from low energy to high energy is shown in Fig. 3(a), and the fitting slopes of 0.72, 0.29, and 0.15 for the three bands give the same conclusion. Accordingly, the presumption of the cause is able to be focused on either an adding factor that is relevant to both energy and z-position, or a multiplying factor that is possibly only relevant to z-position for increasing energy value is capable to produce increasing shift in such a case. This clue is important. Another plot is shown in Fig. 4, which simply transfers the x axis of the plot in Fig. 3(a) to logarithmic scale. It is exciting to find out the similarity of the slopes of the three bands, which suggests that an exponential function of z-position is applicable to neutralize the inclining bands. Therefore, the compensation is performed by employing the following formula,

$$Q_{cor} = Q_1 e^{\lambda_c \cdot R}. \tag{4}$$

Q_t and R are defined in Section 3, λ_c is the slope compensation parameter that can be got by fitting any of the three bands.
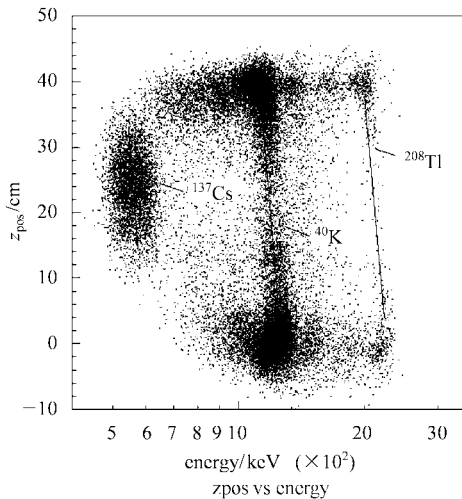

Fig. 4. A logarithmic x axis version of Fig. 3(a). The similar slopes in this plot implies the possibility of the compensation with an exponential function of z-position.

The result is shown in Fig. 5. Apparently, it is easy to conclude even by eyes that the resolution is improved after comparing the plot before and after the compensation. Fitting the second peak by using a gauss function plus a one-order polynomial function as background gives precise figures as depicted in Fig. 5(a). About 36% decreasing of the sigma is

gained. Furthermore, the third ^{208}Tl peak turns out to be much clearer in the second plot, thereby reducing the number of the events that spread to high energy part of the spectra. A 2-D plot after compensation is shown in Fig. 5(b).
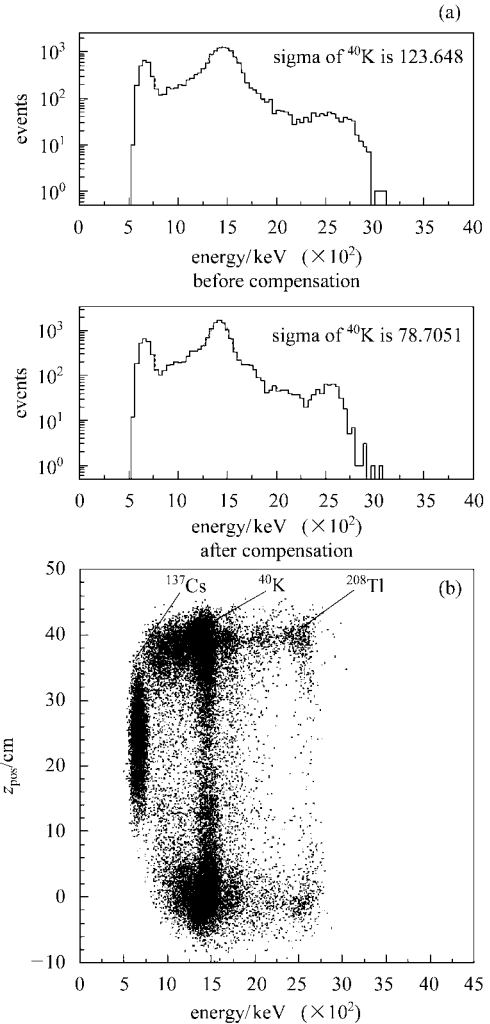

Fig. 5. (a) A comparison of the energy spectra before and after the slope compensation of multiplying an exponential function. A clear improvement can be seen; (b) Plot of z-position versus energy after compensation.

Actually, comparing Eq. (4) with Eq. (2) and Eq. (3), it is not difficult to uncover if the two λ in Eq. (2) and Eq. (3) are not of the same value, Eq. (4) is a natural result that should be applied as compensation.

4.2 Bend compensation

It is not easy to figure out any means to straighten curly bands as displayed in Fig. 3(b). However, some ideas about what kinds of errors may be introduced to our system are already available, one of which is constant bias possibly at-

tached to both Q_l and Q_r due to flaws of the PMTs or the electric system. Fortunately, further study discovers that constant bias does lead to bending. Therefore, a constant bias compensation is employed and a fit function is defined to identify the value.

Actually, according to the idea of the compensation and assuming Q'_l and Q'_l as the true Q value (that means $Q'_l \cdot Q'_r = Q'^2_l = \text{constant}$),

$$Q_t = \sqrt{Q_l \cdot Q_r} = \sqrt{(Q'_l + A)(Q'_r + B)} =$$

$$\sqrt{Q'^2_l + AB + BQ'_r + A \frac{Q'^2_l}{Q'_r}}. \tag{5}$$

From $R' = \dfrac{Q'_r - Q'_l}{Q'_r + Q'_l}$, we can get

$$Q'_r = \frac{1 + R'}{1 - R'} \cdot Q'_l. \tag{6}$$

Make both sides of Equation 6 multiplied by Q'_r and extract their square root

$$Q'_r = r_s \cdot Q'_l, \tag{7}$$

where $r_s = \sqrt{(1 + R')/(1 - R')}$.

To make an approximation that $R' = R = (Q_r - Q_l)/(Q_r + Q_l)$ and substitute Q'_r in Eq. (5) with Eq.(7) to get

$$Q_t = \sqrt{Q'^2_l + AB + BQ'_l \cdot r_s + \frac{AQ'_l}{r_s}}, \tag{8}$$

Where $r_s = \sqrt{(1 + R)/(1 - R)}$.

Here, A, B and Q'_t are all constant and so that a fit base on the plot of Q'_t versus r_s can give the value A and B and hence

$$Q_{cor} = \sqrt{(Q_l - A)(Q_r - B)}. \tag{9}$$

The result is shown in Fig.6(a).

An improvement by about 37% can be obtained to the resolution of ^{40}K peak. As the bands curve toward the low energy part, their two ends can produce a widening effect especially at the low energy side of the peaks to make the left sides evener than the right ones as displayed in the upper plot of Fig. 6(a).

Fig. 6(b) is a 2-D version of the bend compensation result. Though the bands have been straightened comparing to the plot in Fig. 3(b), the bending effect still remains especially at the two ends of the ^{208}Tl band, showing that taking bias as the bend compensation is not a complete solution but a moderate one. A space of further improving the energy spectra still remains in bend compensation.
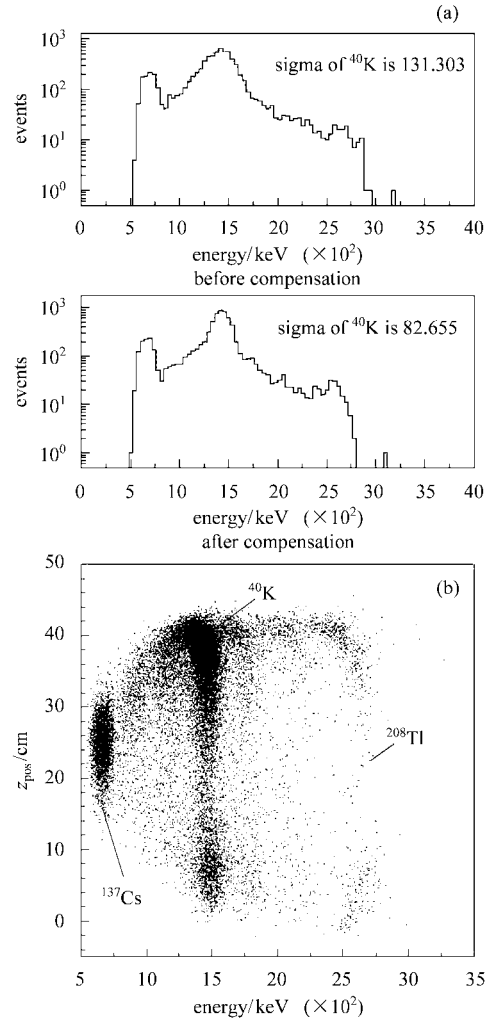

Fig. 6. (a) Constant values are added to Q_l and Q_r as bias compensation. The energy spectra before and after the bend compensation are given here, demonstrating the improvement of the resolution especially at ^{40}K's peak; (b) A 2-D plot of the result of compensation. The bands have been straightened.

5   Summary

This article reviews the data analysis process on CsI(Tl) scintillator detector array in TEXONO experiment. Due to the imperfection in reconstructing energy information, two approaches are developed to improve the resolution of the final energy spectra. Till now, a reactor-OFF data set of 32 crystals has been analyzed for 21 days, and rough calculation of the event rate above 3MeV is performed. As a consequence, we have suppressed the background rate to 0.11 events per day per kg, and thus SNR (neutrino event rate to background event rate) of about 1 : 9 is achieved. Comparison of reactor

ON and OFF spectra as plans can further suppress the background. The goal is to pursue a measurement of the ν_e-e cross section to better than 25% accuracy.

References

1 Wong H T, LI J, Mod. Phys. Lett., 2000, **A15**: 2011
2 LI H B, LIU Y, CHANG C C et al. Nucl. Instrum. Methods, 2001, **A459**: 93
3 Kayser B et al. Phys. Rev., 1979, **D20**: 87
4 Bergsma F et al (CHARM Collaboration). Phys. Lett., 1984, **B147**: 481
5 Vilain P et al (ChARM-Ⅱ Collaboration). Phys. Lett., 1994, **B335**: 246
6 Reines F, Gurr H S, Sobel H W. Phys. Rev. Lett., 1976, **37**: 315
7 Vidyakin G S et al. JETP Lett., 1992, **55**: 206
8 Derbin A I et al. JETP Lett., 1993, **57**: 769
9 Vogel P, Engel J. Phys. Rev., 1989, **D39**: 3378
10 Rosner J L. Phys. Rev., 2004, **D70**: 037301
11 LI H B, Wong H T. J. Phys., 2002, **G28**: 1453
12 LI H B, LI J, Wong H T et al. Phys. Rev. Lett., 2003, **90**: 131802
13 YUE Q et al. Nucl. Instrum. Methods, 2003, **A511**: 408
14 LIU Y, CHEN C P, LI H B et al. Nucl. Instrum. Methods, 2002, **A482**: 125
15 LIU D Z et al. HEP & NP, 2004, **28**(2): 186—190(in Chinese) (刘大治等. 高能物理与核物理, 2004, **28**(2):186—190)

TEXONO 实验中 CsI(Tl)闪烁体探测器阵列的能量与位置重建 *

朱越锋[1;1)]　李玉兰[1]　王子敬[3]　李金[1,2]　Venktesh. Singh[3]　林兴德[3]

1 (清华大学工程物理系　北京　100084)
2 (中国科学院高能物理研究所　北京　100049)
3 (中研院物理所　台北　11529)

摘要　简略叙述了 TEXONO 实验中的数据分析方法. 对于双端读出的 CsI(Tl)晶体探测器的能量重建中出现的两类问题分别提出了补偿方法, 以提高能量谱的分辨率.

关键词　反应堆中微子　CsI(Tl)晶体　分辨率改善